THE FeH WING-FORD BAND IN SPECTRA OF M STARS ⋆

Ricardo P. Schiavon, B. Barbuy & Patan D. Singh

ripisc@atmos.iagusp.usp.br, barbuy@orion.iagusp.usp.br, pdsingh@orion.iagusp.usp.br

Universidade de São Paulo, Instituto Astronômico Geofísico, Departamento de Astronomia

C.P. 9638, São Paulo 01065-970, Brazil

Submitted to: The Astrophysical Journal.

Send proofs to: R. P. Schiavon

⋆ Observations collected at Laboratório Nacional de Astrofísica, Pico dos Dias, Brazil

ABSTRACT

We study the FeH Wing-Ford band at $\lambda\lambda$ 9850 - 10200 Å by means of the fit of synthetic spectra to the observations of M stars, employing recent model atmospheres. On the basis of the spectrum synthesis, we analyze the dependence of the band upon atmospheric parameters. FeH lines are a very sensitive surface gravity indicator, being stronger in dwarfs. They are also sensitive to metallicity (Allard & Hauschildt 1995). The blending with CN lines, which are stronger in giants, does not affect the response of the Wing-Ford band to surface gravity at low resolution (or high velocity dispersions) because CN lines, which are spread all along the spectrum, are smeared out at convolutions of FWHM $\gtrsim$ 3 Å. We conclude that the Wing-Ford band is a suitable dwarf/giant indicator for the study of composite stellar populations.

Subject Headings: Stars: atmospheres, fundamental parameters, M stars - Galaxies: stellar content - Physical data and processes: molecular data.

1. INTRODUCTION

Iron Hydride (FeH) is a typical signature of the atmospheres of the coolest stars. FeH lines have been detected in spectra of M stars (Wing & Ford 1969), S stars (Wing 1972) and sunspots (Carrol & McCormack 1972; Carrol, McCormack & O'Connor 1976). Wing & Ford were the first to detect a band at $\lambda \sim 9900$Å in the spectra of the M dwarfs Wolf 359 and Barnard's star (Gl 699). Nordh, Lindgren & Wing (1977) suggested that the Wing-Ford band was due to FeH, based on the similarity between stellar and laboratory low-resolution spectra. This near infrared (NIR) band was unambiguously assigned to FeH by Wing, Cohen & Brault (1977), through the comparison of sunspot with laboratory high-resolution spectra. As in the case of other hydrides (e.g. MgH, CaH), FeH lines are stronger in dwarfs than in giants.

Whitford (1977) and Carter, Visvanathan & Pickles (1986) attempted to observe the Wing-Ford Band (WFB) in integrated spectra of galaxies, in order to estimate the contribution of M dwarfs to their integrated light, but there was no clear detection of the band. More recently, Hardy & Couture (1988), Davidge (1991) and Couture & Hardy (1993) detected the WFB in integrated spectra of elliptical and lenticular galaxies.

On the laboratory side, the recent years witnessed a large improvement in the knowledge of the structure of FeH. The first laboratory spectrum of FeH was produced by Kleman & Åkerlind (1957, unpublished), but the rotational structure of the line spectrum was not analyzed. Balfour, Lindgren & O'Connor (1983) showed that the WFB was associated to a $^4\Delta - ^4\Delta$ transition. Phillips et al. (1987) carried out a rotational analysis of the WFB, identifying seven vibrational bands and determining rotational and vibrational constants and spin splittings. Langhoff & Bauschlicher (1988) found theoretical evidence in favour of a $^4\Delta$ ground state for FeH. This has been confirmed by recent laboratory results (Carter, Steimle & Brown 1993), which showed that the ground state of FeH is the lower level of the transition associated to the WFB. There is no laboratory determination of the electronic oscillator strenght (f_{el}) of the $A^4\Delta$–$X^4\Delta$ transition.

In this work we compute synthetic spectra for the range of atmospheric parameters of M stars, employing updated model stellar photospheres (Plez et al. 1992; Allard & Hauschildt 1995). These computations are compared to high resolution spectra of M dwarfs and giants in the spectral region of the WFB. Our main interest is to study the behavior of the WFB as a function of stellar parameters, in order to test its usefulness as a discriminator between M giants and dwarfs. In a previous paper (Schiavon et al. 1996), we carried out a similar study applied to the NaI NIR doublet.

In Section 2 the observations are reported. The molecular constants employed are given in Section 3. The computation of synthetic spectra is described in Section 4. In Section 5

the results are discussed. A summary is given in Section 6.

2. OBSERVATIONS

The observations were collected at the coudé focus of the Boller & Chivens 1.6m telescope of the Laboratório Nacional de Astrofísica (LNA), Pico dos Dias, Brazil, in 1995 January and August. A grid of 600 l/mm and a EEV CCD of 770×1152 pixels were used, resulting in a spectral coverage from 9850Å to 10300Å, with a resolution of 0.8Å.

The program stars are listed in Table 1, together with apparent visual magnitudes, spectral types (from Gliese & Jahreiss, 1991, for the dwarfs, and from Hoffleit & Warren, 1991, for the giants), and their effective temperatures and surface gravities, as estimated in Section 2.1.

The spectra were reduced in the usual way; bias subtraction, flatfield correction, spectrum extraction and wavelength calibration were carried out with IRAF routines. Telluric absorption lines were removed through division by the spectra of early-type stars of high $v\sin i$. In Figs. 1a, b we display the spectra of program dwarfs and giants, respectively. The WFB is visible in spectra of dwarfs at $T_{\rm eff} \sim 3700$K, but it becomes strong only for $T_{\rm eff} \leq 3500$K. In spectra of giants FeH lines are not so clearly distinguished because of the blending with CN lines, which are stronger in the spectra of lower gravity stars. In spectra of giants cooler than M5, the TiO bands of the ϵ ($E^3\Pi$–$X^3\Delta$), δ ($b^1\Pi$–$a^1\Delta$) and ϕ ($b^1\Pi$–$d^1\Sigma$) systems (Jorgensen 1994) become apparent and dominate the spectrum of the coolest giant of our sample, HR 1492 (M8).

2.1 Atmospheric Parameters for the Dwarfs

Effective temperatures for the dwarfs were estimated from the ($V–K_{CIT}$) colors compiled by Leggett (1992, hereafter L92), adopting the relation of Jones et al. (1996), where K_{CIT} is defined by Frogel et al. (1978). For two stars (Gl 357 and 842), no K_{CIT} magnitudes are available. In these cases, effective temperatures were estimated from the Cousins (R–I) colors (Bessell 1989), adopting the calibration from Bessell (1990).

The surface gravities were estimated as follows: from the parallaxes and V magnitudes listed by L92 and from the mass *vs.* M_V relation of Henry & McCarthy (1993) we derived stellar masses. Using K_{CIT} and parallaxes from L92, we estimated M_{bol} from the M_{bol} *vs.* M_K relation given by Jones et al. (1996). For Gl 357 and 842, the surface gravities were derived taking M_V from L92, a bolometric correction estimated from Bessell (1990) and the mass *vs.* M_V relation of Henry & McCarthy (1993).

Metallicities are estimated from the stellar populations classification of L92 for M dwarf stars, shown in the last column of Table 1. This classification is based on the kinematic and photometric characteristics (in NIR colors) of a sample of nearby red dwarfs. The stars are divided into five groups: halo stars, old disk/halo stars, old disk stars, old disk/young disk stars and young disk stars.

2.2 Atmospheric Parameters for the Giants

For the giants we derived effective temperatures from the T_{eff} *vs.* spectral type relation from Fluks et al. (1994). As there is no reliable determination of the masses and distances to the giant stars of Table 1, we do not estimate their surface gravities, adopting $\log g$=1.5 to all stars.

3. DETERMINATION OF THE MOLECULAR CONSTANTS

The WFB is due to the $A^4\Delta$–$X^4\Delta$ transition of FeH. The wavelengths of FeH rotational lines for the vibrational transitions (v',v")=(0,0), (0,1), (0,2), (1,0), (1,1), (1,2), (2,0), (2,1) and (2,2) of the $A^4\Delta$–$X^4\Delta$ electronic transition were kindly provided by Dr. J.G. Phillips (Phillips et al. 1987) in digitized format.

3.1 Hönl-London and Franck-Condon Factors

The Hönl-London factors were computed using the code by Whiting & Nicholls (1973), which was kindly made available to us by Dr. J. Brown.

The Franck-Condon factors ($q_{v'v''}$) were computed with the program for transition probabilities of molecular transitions written by Jarmain & McCallum (1970). The observed energy levels (E_v) and rotational constants for the two participating electronic states of the FeH molecule are from the laboratory analyses of Carter et al. (1993) and Phillips et al. (1987). The minimum and maximum integration limits for the wavefunctions of both electronic states were fixed at 1.42 and 6.62$bohr$, respectively. Since $r'_e \sim r''_e$, strong bands lie on the Δv=0 sequence. For the dissociation energy, we adopted a recent laboratory determination from Schulz & Armentrout (1991), D_0=1.63eV. In Table 2 we present the $q_{v'v''}$ and r-centroids for the FeH $A^4\Delta$–$X^4\Delta$ system. Since

$$\sum_{v'} q_{v'0} \sim 1,$$

direct photodissociation of the molecule is not possible through the $A^4\Delta$ state.

3.2 Electronic Oscillator Strength

We adopted an empirical value for the electronic oscillator strength of the $A^4\Delta$–$X^4\Delta$ transition, requiring consistency between the model photospheres employed and the observa-

tions. One of our program stars (Gl 699) was studied by Jones et al. (1996), who determined the stellar atmospheric parameters of a number of M dwarfs from spectrum synthesis of low resolution spectra in the NIR, curves of growth of atomic lines and kinematic data. Their analysis was based on an improved version of the Allard & Hauschildt (1995) model photospheres. For Gl 699, they found T_{eff}=3200K, $\log g$=5.0 and –1.5<[Fe/H]<–1.0. We fitted the observed intensity of the WFB in Gl 699 with a synthetic spectrum computed with T_{eff}=3200K, $\log g$=5.0 and [Fe/H]=–1.0, having obtained $f_{el} \sim 1 \times 10^{-3}$. This value is one order of magnitude lower than the value proposed by Langhoff & Bauschlicher (1990), on the basis of *ab initio* calculations.

3.3 Dissociative Equilibrium Constant

The dissociative equilibrium was computed following Tsuji (1973). The dissociative equilibrium constant of FeH as a function of reciprocal temperature (θ=5040K/T) $K_{FeH}(\theta)$, is not available in the work of Tsuji (1973). We computed $K_{FeH}(T)$ from equation (7) of Tatum (1966). The molecular partition function as a function of temperature, $Q_{FeH}(T)$, was computed from equation (15) of Tatum (1966), taking the electronic terms, the rotational, vibrational and anharmonicity constants from Phillips et al. (1987). For the partition function of Fe as a function of temperature, we adopted the polynomial fit given by Irwin (1981). The function $K_{FeH}(\theta)$ thus obtained was fitted by a fourth order polynomial as follows:

$$\log K_{FeH}(\theta) = \sum_{i=0}^{4} a_i \theta^i$$

where $(a_0, a_1, a_2, a_3, a_4)$=(12.867,–3.8754,1.0326,–0.22476,0.01775). Our calculations show that the region of the WFB in the spectra of M stars is dominated by FeH, CN and atomic lines. The CN lines due to the (1,0), (2,1) and (3,2) vibrational bands of the $A^2\Pi - X^2\Sigma$ transition were taken from the work of Davis & Phillips (1963).

4. SPECTRUM SYNTHESIS

The synthetic spectra were computed in the interval $\lambda\lambda 9850 - 10200$Å. The spectrum synthesis code used is described in Barbuy (1982). The model photospheres adopted are from Allard & Hauschildt (1995) for the dwarfs and from Plez et al. (1992) for the giants. The atomic line list was taken from Swensson et al. (1973), with oscillator strengths and damping constants obtained by fitting the solar spectrum (Kurucz et al. 1984), adopting the solar model photosphere of Kurucz (1992). For the line profiles we adopted the Hjerting function.

4.1 Dwarfs

We computed synthetic spectra for a grid of 157 model photospheres in the range of atmospheric parameters $2700 \leq T_{\rm eff} \leq 4000$K, $4.0 \leq \log g \leq 5.5$ and $-1.5 \leq$ [Fe/H] $\leq +0.5$. In Fig. 2 are shown synthetic spectra computed for $T_{\rm eff}$=3200K, $\log g$=5.0 and solar metallicity, with: a) CN lines only, b) atomic lines only and c) FeH, CN and atomic lines.

Adopting the atmospheric parameters given in Table 1, we obtained a good match between synthetic and observed spectra for 8 of the program dwarf stars. Two of the remaining 5 stars (Gl 357 and 842) are not included in the list of L92, so that we do not have estimates for their metallicities. For the other three stars (Gl 1, 190 and 285), the synthetic spectra did not match the observed ones.

In Fig. 3a we show, as a typical example, the comparison of spectrum synthesis and observation for Gl 699. The good agreement between synthetic and observed spectra for the majority of the program stars validates our choice of the empirical value of the electronic strength for the $A^4\Delta$– $X^4\Delta$ transition of FeH.

For Gl 1, 190 and 285, we improved the estimate of the atmospheric parameters in three steps:

i) For each star we computed the *rms* deviation of each synthetic spectrum of our grid relative to the observed spectrum and selected the best 20% synthetic spectra.

ii) We measured the depth ratios of a set of lines selected on the basis of their sensitivity to atmospheric parameters. The lines used are listed in Table 3, together with the identification of the contributors to the absorption. All the line ratios present a strong sensitivity to at least one of the three atmospheric parameters (Figs. 4a,b), so that the set of 10 pairs can be used as a further constraint to select the atmospheric parameters. We require that the difference between the observed and synthetic line ratios be of the order of the uncertainties in the measurements (usually $\sim$ 10-20%). The uncertainties are estimated using the expression of Gray & Johansson (1991).

iii) The resulting values of $T_{\rm eff}$, $\log g$ and [Fe/H] are finally compared to those of Table 1, requiring that $\Delta T_{\rm eff} < \pm 300$K, $\Delta \log g < \pm 0.5$ and Δ[Fe/H] $< \pm 0.5$.

After the selection process, there remained five sets of distinct atmospheric parameters per star, on average. These final atmospheric parameters were averaged and the resulting values are shown in Table 4. In order to check the reliability of this method, it was applied to the 8 stars for which the synthetic spectra based on the atmospheric parameters of Table 1 presented a good fit to the observations. By comparing the values of Tables 1 and 4, it is seen that the differences in $T_{\rm eff}$, $\log g$ and [Fe/H] for these 8 stars are smaller than 150K, 0.2 and 0.4 dex, respectively. In Figs. 3b,c we show the comparison of synthetic and observed spectra for Gl 1 and 285, which are, respectively, the hotter and cooler star in our sample.

4.2 Giants

In Fig. 5 we show the spectrum synthesis for the giant star HR 832 (M4), where the atmospheric parameters adopted are ($T_{\rm eff}$,$\log g$,[Fe/H]) = (3400K,1.5,0.0).

CN lines become important in the spectra of giants, as illustrated in Fig. 6, where the separate contributions of molecular and atomic lines are shown for stellar parameters T_{eff}=3600K, $\log g$=1.5 and solar metallicity (compare with Fig. 2, for the case of dwarfs). Because CN lines are more important in the spectra of giants, they change the response of the equivalent width of the WFB to atmospheric parameters.

5. THE WING-FORD BAND AS A FUNCTION OF ATMOSPHERIC PARAMETERS AND SPECTRAL RESOLUTION

The equivalent width of the WFB was measured in the 157 synthetic spectra of the grid, in the interval $\lambda\lambda$ 9896-9980 Å, with continuum points located at the endpoints of this interval.

The equivalent width measured in spectra of giants has an important contribution from CN lines (Fig. 6). This contribution is a strong function of the resolution of the spectrum. In Fig. 7 we show the synthetic spectrum due to CN only, for a giant of T_{eff}=3600K convolved with gaussians of FWHM=0.8 and 5Å. From this Fig. it is seen that, since CN lines are spread all along the spectral region, showing no pronounced features, their presence is diluted at lower resolutions. Therefore, the main effect of CN lines at low resolution is the lowering of the pseudo-continuum adjacent to the WFB. Therefore, we convolved our grid of synthetic spectra with gaussians of different FWHM, in order to study the effect of resolution upon the equivalent width measurements.

5.1 Behavior of WFB at High Resolution

In Fig. 8 we show the equivalent width of the WFB as a function of effective temperature and surface gravity, computed for FWHM=0.8Å. As expected, the WFB is very sensitive to both parameters. There is a clear distinction between the behavior of giants and dwarfs. In

dwarfs FeH lines are predominant whereas CN lines are stronger in giants.

In the dwarf regime, the WFB behaves as expected, for $T_{eff} \leq 3300$K, it becomes stronger for higher $\log g$. (It has to be noted that for higher temperatures, there is an inversion of this trend for the models at $\log g$=4.0 and 4.5. The same inversion happens for the models at $\log g$=4.5 and 5.0 at $T_{eff} \sim$ 3500K. This inversion is presumably due to the effect pointed out by Brett (1995, his Fig. 3), concerning the decreasing importance of convective transport for decreasing gravities, and the influence of convection on the temperature gradient of the photosphere. The effect does not appear in lower T_{eff} models because the efficiency of convective transport reaches a maximum at $T_{eff} \sim$ 3200K).

In Fig. 9 we show the behavior of the WFB equivalent width as a function of effective temperature and metallicity for dwarfs. (This plot shows the unexpected behavior of stronger FeH lines at lower metallicities. This effect was already pointed out by Allard & Hauschildt (1995) and is related to the increased gas pressure of metal poor photospheres, at a given optical depth, which overcompensates the lower particle number density; the same result is obtained using Kurucz (1992) model photospheres for T_{eff}=3500K. For T_{eff} >3300K, the trend begins to change for higher metallicities, so that the band assumes the usual behavior for $T_{eff} \sim$4000K).

In the giants CN lines dominate the WFB equivalent width; CN lines are stronger for lower $\log g$ and higher T_{eff} (the latter being valid for $T_{eff} < 4400$ K, cf. Milone & Barbuy 1994).

5.2 Behavior of WFB at Low Resolution

In Figs. 10a to 10d we show the dependence of the WFB on T_{eff} and $\log g$ for spectra convolved with gaussians of increasing FWHM. For FHWM=2Å, the dependence of WFB on gravity is not significantly different from what is seen in Fig. 8. As convolution increases, the pseudo-continuum level decreases in the spectra of giants, leading to lower WFB equivalent

widths. The effect is more important for lower resolution (higher FWHM) and stronger CN lines. Hence, while the WFB equivalent width in dwarfs is almost invariant with convolution, it is sensibly lower in giants for higher FHWM. Therefore, the WFB is a suitable dwarf/giant discriminator at lower resolutions, where the blend of CN inside the interval $\lambda\lambda$ 9896-9980Å is compensated by the lowering of the adjacent pseudo-continuum due to unresolved CN lines.

Stellar velocity dispersions in elliptical galaxies are around $50 < \sigma < 350$ km/s (e.g. Ore et al. 1991), which corresponds to $0.9 <$ FWHM < 6 Å. Based on this discussion, it appears that the WFB is an appropriate indicator of cool dwarf populations for galaxies with $\sigma \gtrsim 200$km/s. For galaxies of lower σ the WFB observed in lower resolution can also be used as a dwarf-giant discriminator.

6. SUMMARY

We computed synthetic spectra for a range of atmospheric parameters, using state-of-the-art model photospheres, in the interval $\lambda\lambda 9850 - 10200$Å. This region includes the Wing-Ford band (WFB) of FeH, which is a well known surface gravity indicator.

Based on a set of atmospheric parameters derived from photometric indices and kinematic population classifications, we compared our synthetic spectra with observations of M dwarf stars, obtaining a satisfactory match.

The equivalent width of the WFB was studied as a function of effective temperature, surface gravity, metallicity and spectral resolution. FeH lines are dominant in the spectra of dwarfs. For dwarfs cooler than 3500K, the dependence of the equivalent width of the WFB on $\log g$ follows the expected trend, being higher for higher $\log g$ and lower $T_{\rm eff}$.

CN lines become dominant in spectra of giants, however at convolutions of FWHM $\gtrsim 3$ Å the CN lines, which are spread all along the spectrum are smoothed out, with the main

effect of lowering the pseudo-continuum. The same effect occurs for velocity dispersions of stars in galaxies where $\sigma \gtrsim 200$km/s, i.e., the CN lines present in giants are smeared out.

We conclude that the Wing-Ford is a suitable dwarf/giant indicator for the study of stellar populations in external galaxies.

The authors are indebted to B. Plez and F. Allard for kindly providing their model atmospheres, Dr. J. Phillips for the line list of FeH and Dr. J. Brown for the code for the computation of Hönl-London factors. We also thank the referee, P. Hauschildt, for his suggestions on the first version of the manuscript. The calculations were carried out in a DEC Alpha 3000/700 workstation provided by Fapesp. RPS acknowledges Fapesp PhD fellowship No. 93/2177-0. Partial financial support from CNPq is also acknowledged.

REFERENCES

Allard, F. & Hauschildt, P.H., 1995, ApJ, 445, 433.

Balfour, W.J., Lindgren, B. & O'Connor, S., 1983, Chem.Phys.Lett., 96, 251.

Barbuy, B., 1982, PhD thesis, Université de Paris VII.

Bessell, M.S., 1990, A&AS, 83, 357.

Bessell, M.S., 1991, AJ, 101, 662.

Brett, J.M., 1995, A&A, 295, 736.

Carrol, P.K. & McCormack, P., 1972, ApJ, 177, L33.

Carrol, P.K., McCormack, P. & O'Connor S., 1976, ApJ, 208, 903.

Carter, R.T., Steimle, T.C. & Brown, J.M., 1993, J.Chem.Phys, 99, 3166.

Carter, D., Visvanathan, N. & Pickles, A.J., 1986, ApJ, 311, 637.

Couture, J. & Hardy, E., 1993, ApJ, 406, 142.

Davis, S.P. & Phillips, J.G., 1963, The red system ($A^2\Pi - X^2\Sigma$) of the CN molecule, Univ. California Press.

Fluks, M.A., Plez, B., Thé, P.S., de Winter, D., Westerlund, B.E. & Steenman, H.C., 1994, A&AS, 105, 311.

Frogel, J.A., Persson, S.E., Aaronson, M. & Matthews, K. 1978, ApJ, 220, 75.

Gliese, W & Jahreiss, H., 1991, Preliminary Version of the Third Catalogue of Nearby Stars, Astronomisches Rechen-Institute Heidelberg, Germany.

Gray, D.F., Johanson, H.L., 1991, PASP, 103, 439.

Hardy, E. & Couture, J., 1988, ApJ, 325, L29.

Henry, T.J. & McCarthy, Jr., D.W., 1993, AJ, 106, 773.

Hoffleit, D. & Warren Jr., W.H., 1991, Preliminary Version of the Bright Star Catalogue, 5th Revised Edition.

Irwin, A.W., 1981, ApJS, 45, 621.

Jarmain, W.R. & McCallum, J.C., 1970, TRAPRB, University of Western Ontario, Dept. of Physics, Ontario, Canada.

Jones, H.R.A., Longmore, A.J., Allard, F. & Hauschildt, P.H., 1996, MNRAS, 280, 77.

Jorgensen, U.G.: 1994, A&A, 284, 179.

Kurucz, R., 1992, in The Stellar Populations of Galaxies, IAU Symp. 149, eds. B. Barbuy & A. Renzini, Kluwer Acad. Press, 225

Kurucz, R.L., Furenlid, I., Brault, J., Testerman, L., 1984, Solar Flux Atlas from 296 to 1300 nm (Sunspot, N.M., National Solar Observatory).

Langhoff, S.R. & Bauschlicher, C.W.Jr., 1988, J.Chem.Phys., 89, 2160.

Langhoff, S.R. & Bauschlicher, C.W.Jr., 1990, J.Mol.Spectrosc., 141, 243.

Leggett, S.K., 1992, ApJS, 82, 351 (L92).

Milone, A. & Barbuy, B., 1994, A&AS, 108, 449.

Nordh, H.L., Lindgren, B. & Wing, R.F., 1977, A&A, 56, 1.

Ore, C.D., Faber, S.M., Jesus, J., Stoughton, R., 1991, ApJ, 366, 38

Plez, B., Brett, J.M. & Nordlund, A., 1992, A&A, 256, 551.

Phillips, J.G., Davis, S.P., Lindgren, B. & Balfour, W.J., 1987, ApJS, 65, 721.

Schiavon, R.P., Barbuy, B., Rossi, S.C.F. & Milone, A., 1996, ApJ, in press.

Schultz, R.H. & Armentrout, P.B., 1991, J.Chem.Phys., 94, 2262.

Spinrad, H. & Taylor, B.J., 1971, ApJS, 22, 445.

Swensson, J.W., Benedict, W.S., Delbouille, L. & Roland, G., 1973, Mém. Soc. R. Sci. Liège Special, vol. 5.

Tatum, J.B., 1966, Pub. Dom. Ap. Obs. Victoria, 13, 1.

Tsuji, T., 1973, A&A, 23, 411.

Whitford, A.E., 1977, ApJ, 21, 527.

Whiting, E.E. & Nicholls, R.W., 1973, ApJS, 27, 1.

Wing, R.F., 1972, Mem. Soc. R. Sci. Liège, Ser.3, 123.

Wing, R.F., Cohen, J. & Brault, J.W., 1977, ApJ, 216, 659.

Wing, R.F. & Ford, W.K., 1969, PASP, 81, 527.

Table 1 - Program Stars. Visual Magnitudes, spectral types, effective temperatures, surface gravities and population class. The population classification was taken from Leggett (1992): halo stars (H), old disk/halo stars (O/H), old disk stars (OD), old disk/young disk stars (O/Y) and young disk stars (YD). Metallicities for each class are as follows: $[Fe/H]_{H}$ ∼–1.0, $[Fe/H]_{O/H}$ ∼–1.0, $[Fe/H]_{OD}$ ∼–0.5, $[Fe/H]_{O/Y}$ ∼–0.5, $[Fe/H]_{YD}$ ∼0.0. For the derivation of the other atmospheric parameters, see Section 2.1.

star	V	Sp.T.	T_{eff}(K)	log g	Class
			Dwarfs		
Gl 1	8.54	M4	3460	4.9	H
Gl 84	10.19	M3	3320	4.7	OD
Gl 190	10.30	M4	3180	4.3	YD
Gl 229	11.2	M1e	3480	4.6	Y/O
Gl 273	9.85	M3.5	3170	4.8	OD
Gl 285	11.2	M4.5e	3080	4.6	YD
Gl 357	10.92	M3	3410	4.6	
Gl 581	10.56	M5	3240	4.9	YD
Gl 699	9.55	M5	3160	5.1	O/H
Gl 752 A	9.11	M3.5e	3310	4.7	Y/O
Gl 832	8.67	M1	3400	4.8	O/H
Gl 842	9.75	M2	3640	4.7	
Gl 876	10.17	M5	3140	4.7	YD
			Giants		
HR625	6.10	M2	3740		
HR722	6.41	M5	3430		
HR832	6.90	M4	3570		
HR1492	5.40	M8	2890		
HR1693	5.68	M6	3310		
HR8128	5.28	M3	3670		

Table 2 - Franck-Condon factors (first entry) and r-centroids (second entry) of the $A^4\Delta$–$X^4\Delta$ transition of FeH

v''	0	1	2
v'			
0	8.33×10^{-1}	1.56×10^{-1}	1.06×10^{-2}
	1.671	1.938	2.180
1	1.46×10^{-1}	5.52×10^{-1}	2.70×10^{-1}
	1.456	1.720	1.992
2	1.73×10^{-2}	2.16×10^{-1}	2.99×10^{-1}
	1.252	1.511	1.782

Table 3 - Line Pairs

$\lambda_{\rm obs}$	Identification	$\chi_{\rm exc(eV)}/(v',v'')Branch-J$
9899.1	FeH 9899.22	$(0,0)R-15$
	FeH 9899.33	$(0,0)P-10$
	CN 9899.16	$(1,0)P_1-55$
9900.9	CrI 9900.95	2.99
	CN 9900.79	$(3,2)Q_1-34$
9926.3	FeH 9926.41	$(0,0)R-12$
9927.4	TiI 9927.38	1.88
	FeH 9927.37	$(0,0)R-6$
	FeH 9927.37	$(0,0)R-10$
	CN 9927.49	$(3,2)Q_1-36$
9931.7	CaII 9931.35	7.51
	FeH 9931.59	$(0,0)R-7$
	FeH 9931.79	$(0,0)R-3$
9933.3	SI 9932.37	8.41
	FeH 9933.29	$(0,0)R-13$
9959.6	FeI 9959.17	4.07
	FeH 9959.63	$(0,0)R-7$
9961.1	NaI 9961.25	3.62
	FeH 9961.14	$(0,0)P-16$
10007.0	FeI 10007.32	3.02
10010.3	FeH 10010.45	$(0,0)R-9$
10010.3	FeH 10010.45	$(0,0)R-9$
10012.1	FeI 10012.20	5.07

Table 3 - Continuation

$\lambda_{\rm obs}$	Identification	$\chi_{\rm exc(eV)}/Branch-J$
10033.1	FeI 10032.89	5.50
	FeH 10033.07	$(0,0)R-22$
10035.7	FeH 10035.60	$(0,0)R-26$
	CN 10035.77	$(1,0)Q_1-68$
10074.1	FeH 10074.04	$(0,0)R-22$
	CN 10074.07	$(3,2)Q_1-45$
10075.1	FeH 10075.22	$(0,0)P-17$
	FeH 10075.22	$(0,0)P-6$
10187.7	FeH 10187.66	$(0,0)P-11$
	CN 10187.86	$(2,1)Q_1-63$
10189.3	TiI 10189.02	1.46
10194.8	FeI 10195.12	2.73
	FeH 10194.71	$(0,0)P-11$
10196.3	FeH 10196.22	$(0,0)P-10$
	CN 10196.47	$(2,1)P_2-56$

Table 4 - Best Set of Atmospheric Parameters for Program M Dwarfs

Star	T_{eff}(K)	log g	[Fe/H]
Gl 1	3650	4.9	−1.1
Gl 84	3210	4.9	−0.6
Gl 190	2900	4.4	−0.2
Gl 229	3330	4.7	−0.2
Gl 273	3180	4.8	−0.8
Gl 285	2830	5.0	−0.3
Gl 357	3190	4.7	−1.0
Gl 581	3230	5.1	−0.1
Gl 699	3260	5.2	−0.9
Gl 752 A	3370	4.8	−0.8
Gl 832	3320	4.7	−0.7
Gl 842	3410	4.8	−0.6
Gl 876	3130	4.9	−0.4

FIGURE CAPTIONS

Figure 1a: Spectra of program M dwarfs showing the Wing-Ford band in high resolution ($\sim \lambda\lambda 9900 - 10000$Å). Effective temperatures range between $\sim$ 2800K (Gl 285) to $\sim$ 3700K (Gl 1).

Figure 1b: Spectra of program M giants. Effective temperatures range between $\sim$ 2900K (HR 1492) to $\sim$ 3700K (HR 625).

Figure 2: Separate contribution of CN, atomic and FeH lines for the spectrum of a dwarf M star.

Figure 3a: Spectrum synthesis of Gl 699 (Barnard's Star).

Figure 3b: Spectrum synthesis of Gl 1.

Figure 3c: Spectrum synthesis of Gl 285.

Figure 4a: Line depth ratio of a line pair of Table 3 as a function of $T_{\rm eff}$ and $\log g$, computed for solar metallicity.

Figure 4b: Line depth ratio of a line pair of Table 3 as a function of $T_{\rm eff}$ and metallicity, computed for $\log g$=5.0.

Figure 5: Spectrum synthesis of HR 832.

Figure 6: Separate contribution of CN, atomic and FeH lines for the spectrum of a giant M star.

Figure 7: CN line spectrum for a giant of $T_{\rm eff}$=3600K, $\log g$=1.0 and solar metallicity, convolved with gaussians of FWHM=0.8Å (dotted line) and 5.0Å (solid line).

Figure 8: Equivalent width of the Wing-Ford band as a function of $T_{\rm eff}$ for different gravities. The synthetic spectra were convolved with a gaussian of FWHM=0.8Å.

Figure 9: Equivalent width of the Wing-Ford band as a function of $T_{\rm eff}$ for different metallicities. The synthetic spectra were convolved with a gaussian of FWHM=0.8Å.

Figure 10: Equivalent width of the Wing-Ford band as a function of $T_{\rm eff}$ for different

gravities. Each panel corresponds to a distinct convolution of the synthetic spectra: a) FWHM=2.0Å, b) 3.0Å, c) 4.0Å and d) 5.0Å. The discrimination between dwarfs and giants increases for increasing FWHM.

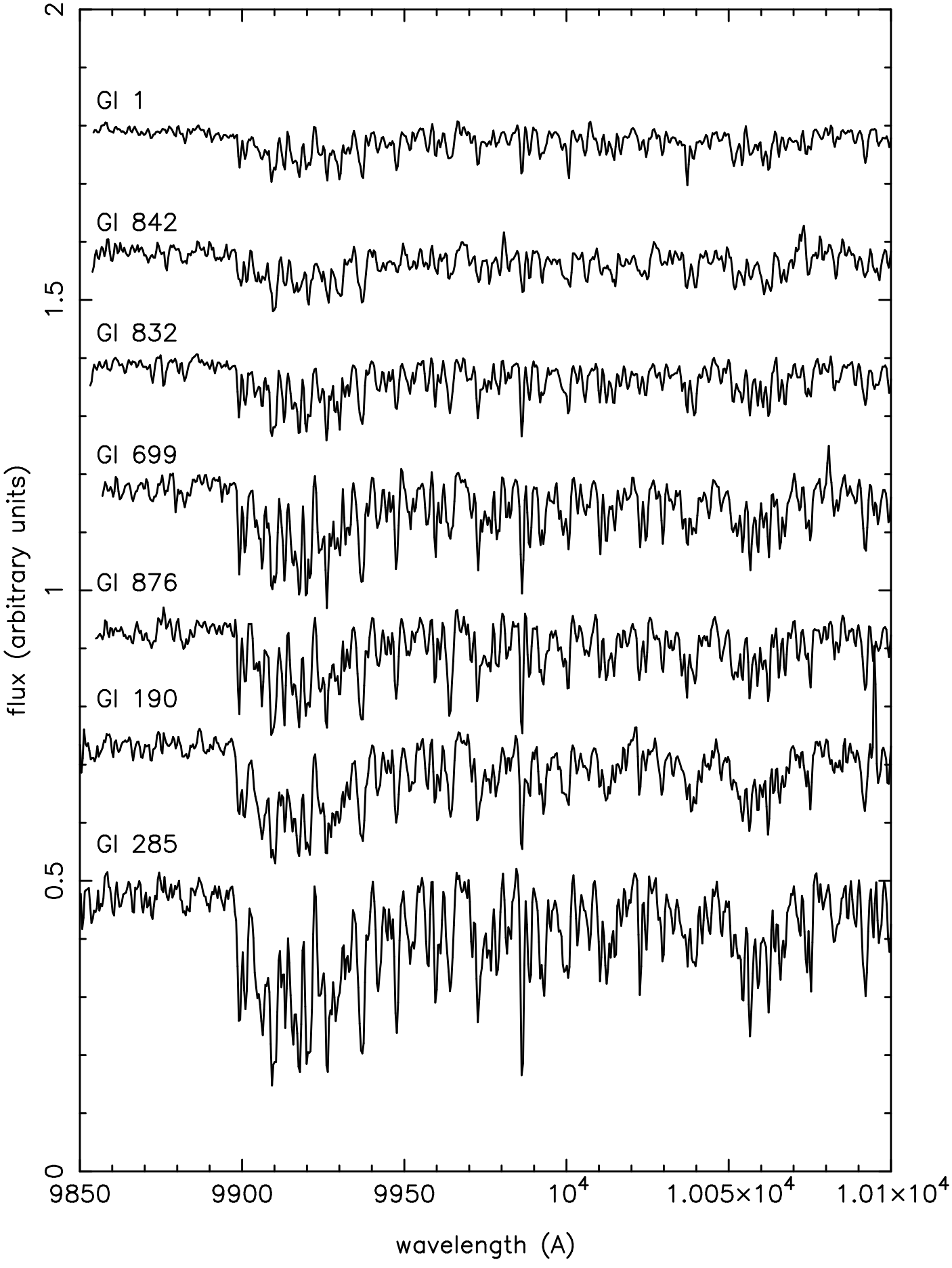
Gl 1
Gl 842
Gl 832
Gl 699
Gl 876
Gl 190
Gl 285
flux (arbitrary units)
0
0.5
1
1.5
2
9850
9900
9950
10^4
1.005×10^4
1.01×10^4
wavelength (A)

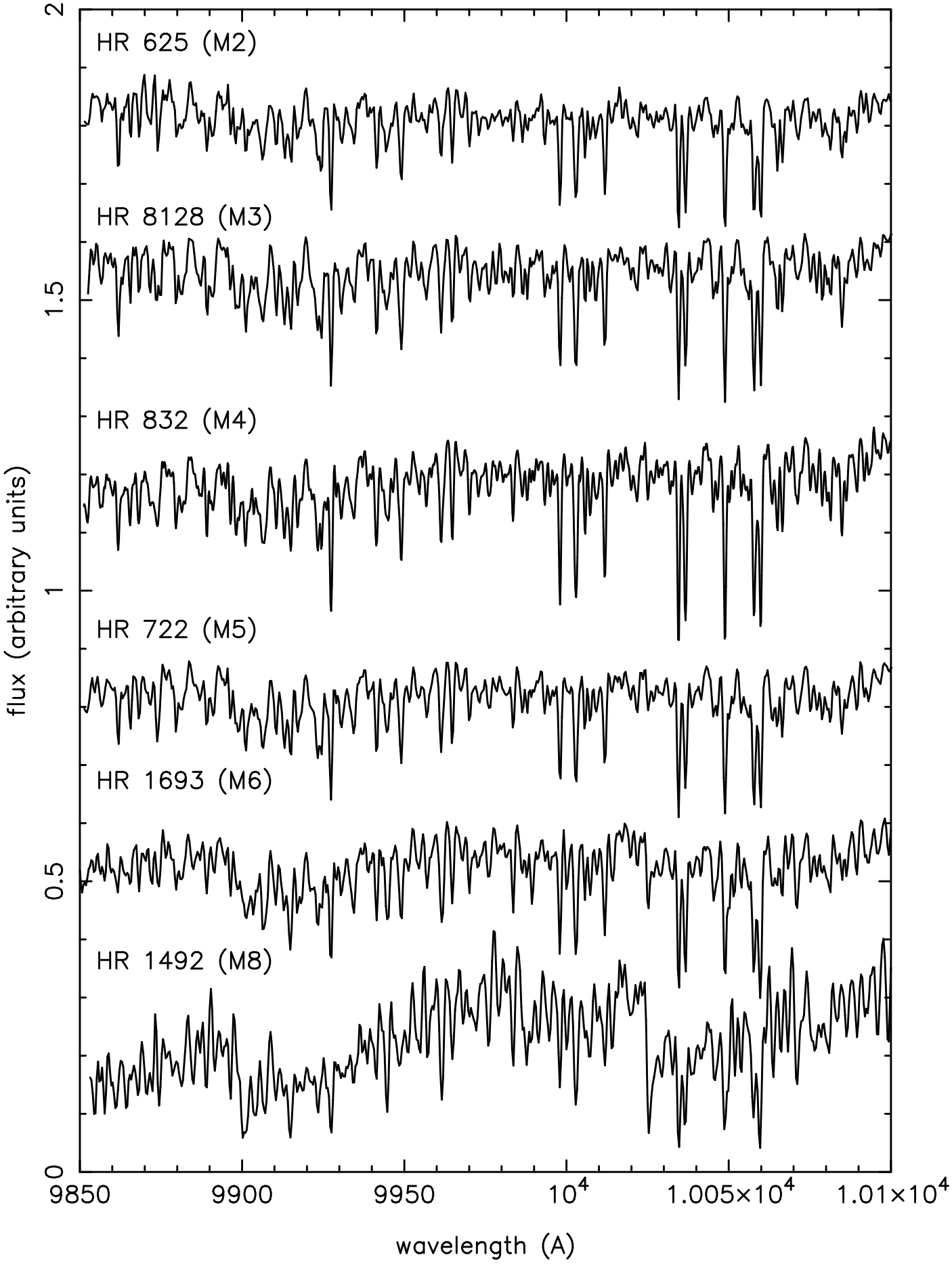
HR 625 (M2)
HR 8128 (M3)
HR 832 (M4)
HR 722 (M5)
HR 1693 (M6)
HR 1492 (M8)
flux (arbitrary units)
0
0.5
1
1.5
2
9850
9900
9950
10^4
1.005×10^4
1.01×10^4
wavelength (A)

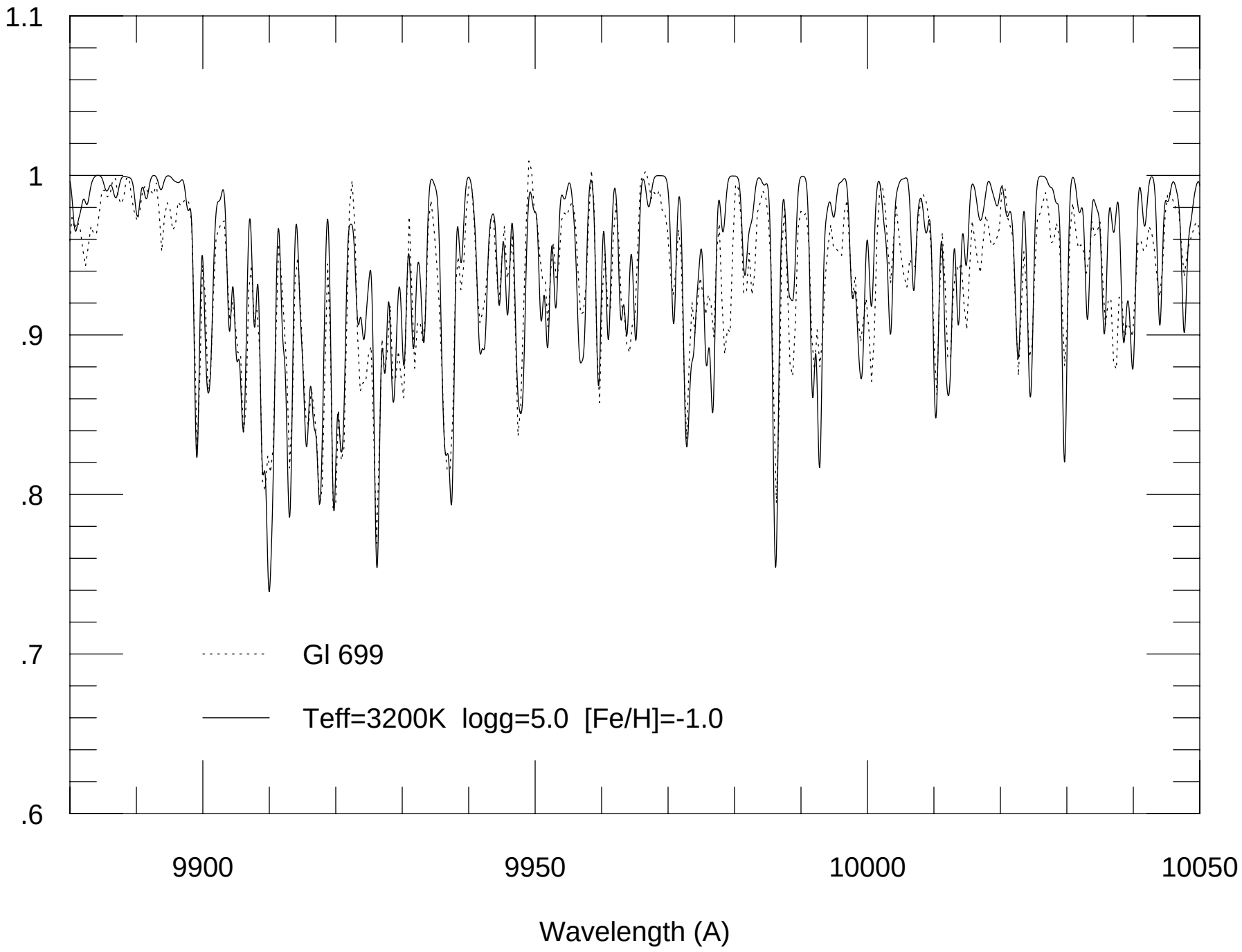
1.1
1
.9
.8
.7
.6
9900
9950
10000
10050
Wavelength (A)
Gl 699
Teff=3200K logg=5.0 [Fe/H]=-1.0

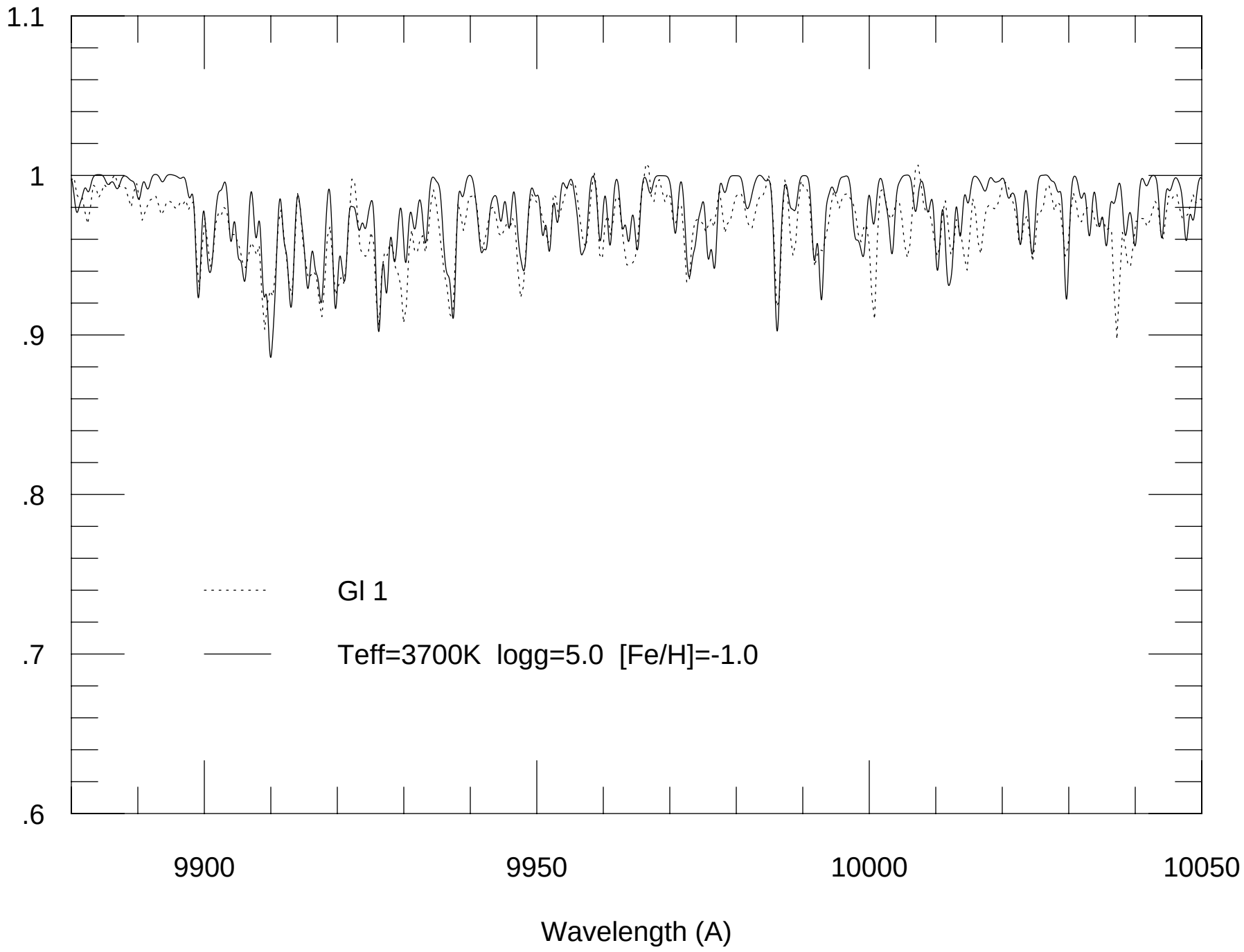
1.1
1
.9
.8
.7
.6
9900
9950
10000
10050
Wavelength (A)
Gl 1
Teff=3700K logg=5.0 [Fe/H]=-1.0

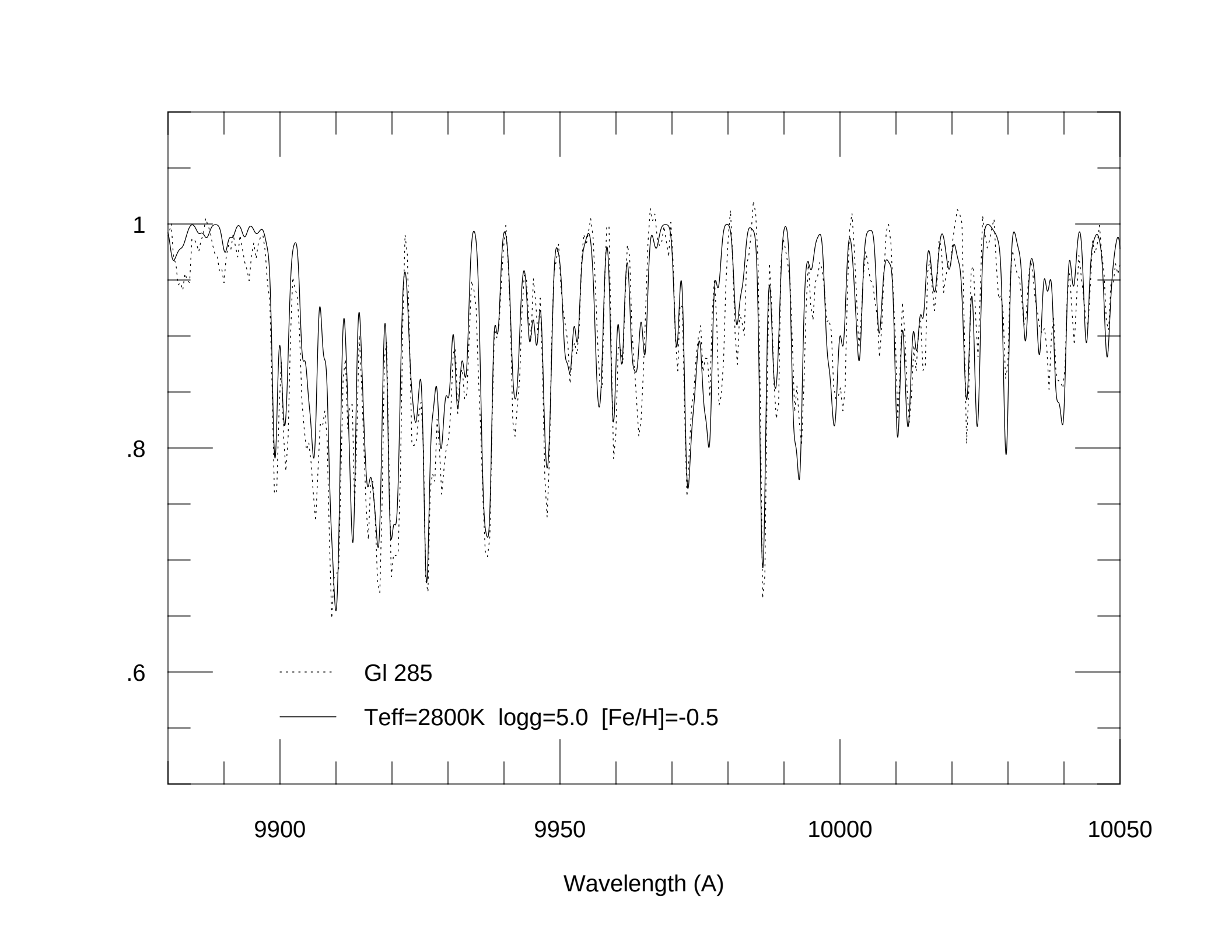
1
.8
.6
Gl 285
Teff=2800K logg=5.0 [Fe/H]=-0.5
9900
9950
10000
10050
Wavelength (A)

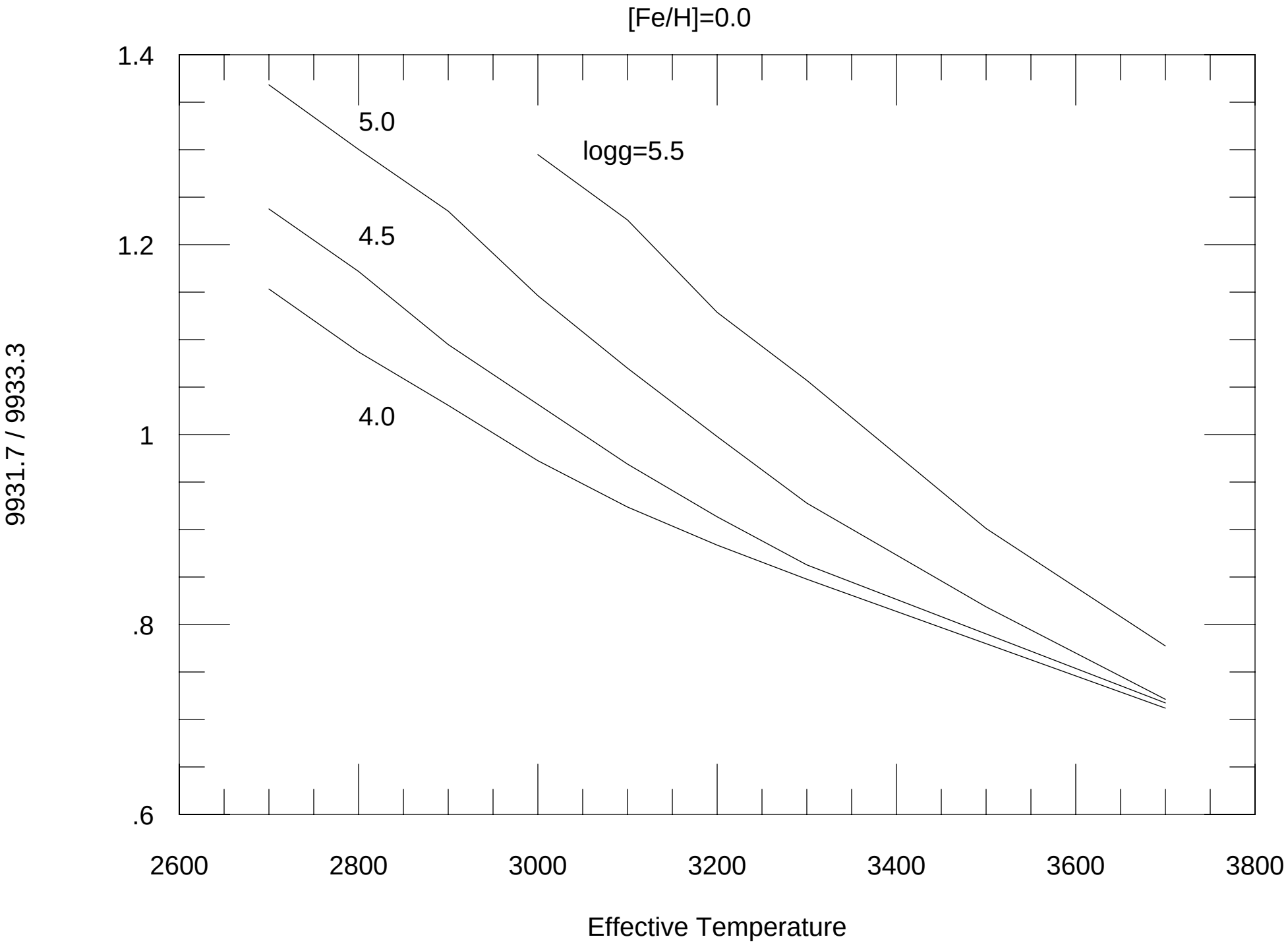
[Fe/H]=0.0
1.4
1.2
1
.8
.6
9931.7 / 9933.3
5.0
logg=5.5
4.5
4.0
2600
2800
3000
3200
3400
3600
3800
Effective Temperature

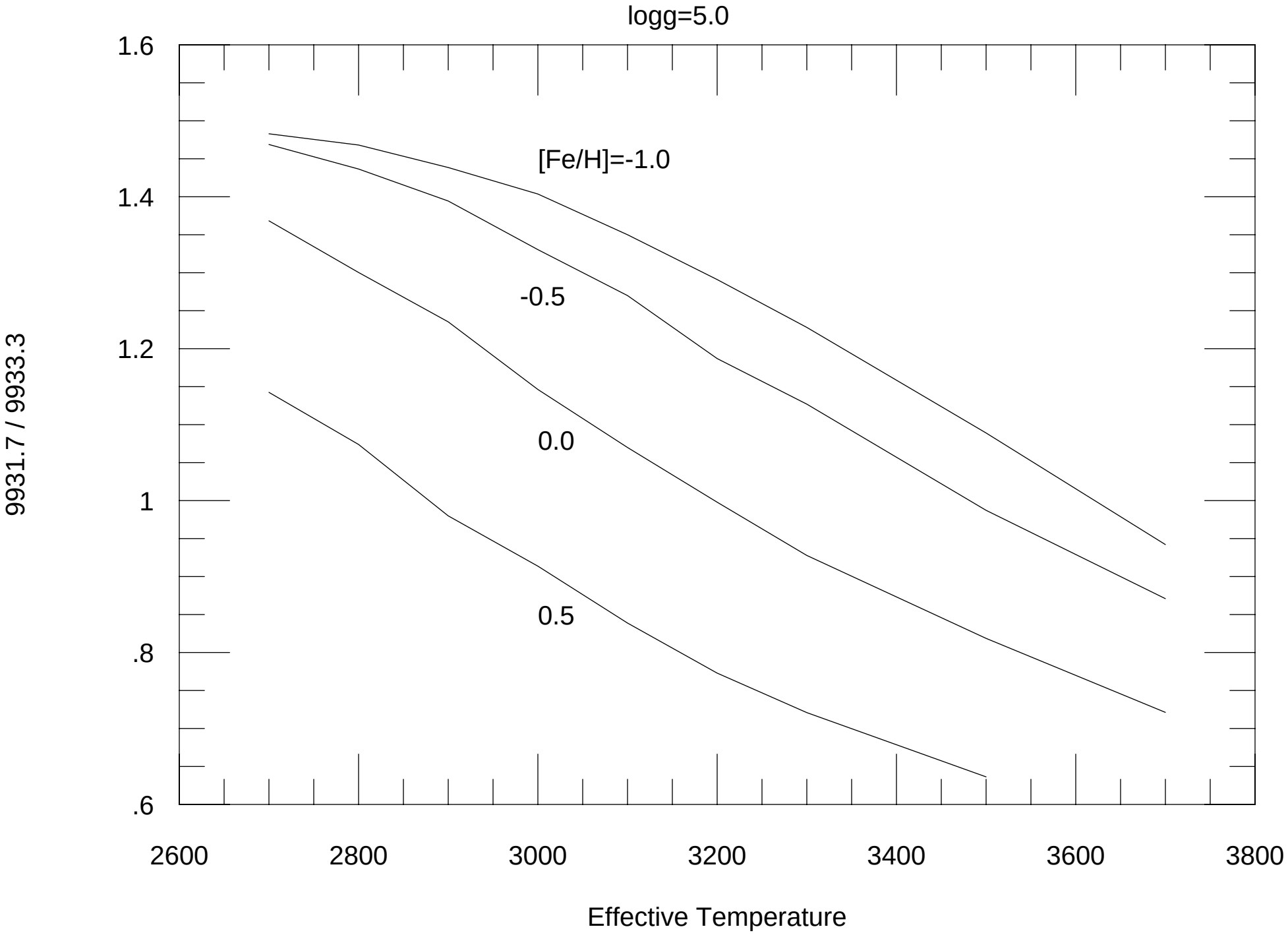
logg=5.0
[Fe/H]=-1.0
-0.5
0.0
0.5
1.6
1.4
1.2
1
.8
.6
9931.7 / 9933.3
2600
2800
3000
3200
3400
3600
3800
Effective Temperature

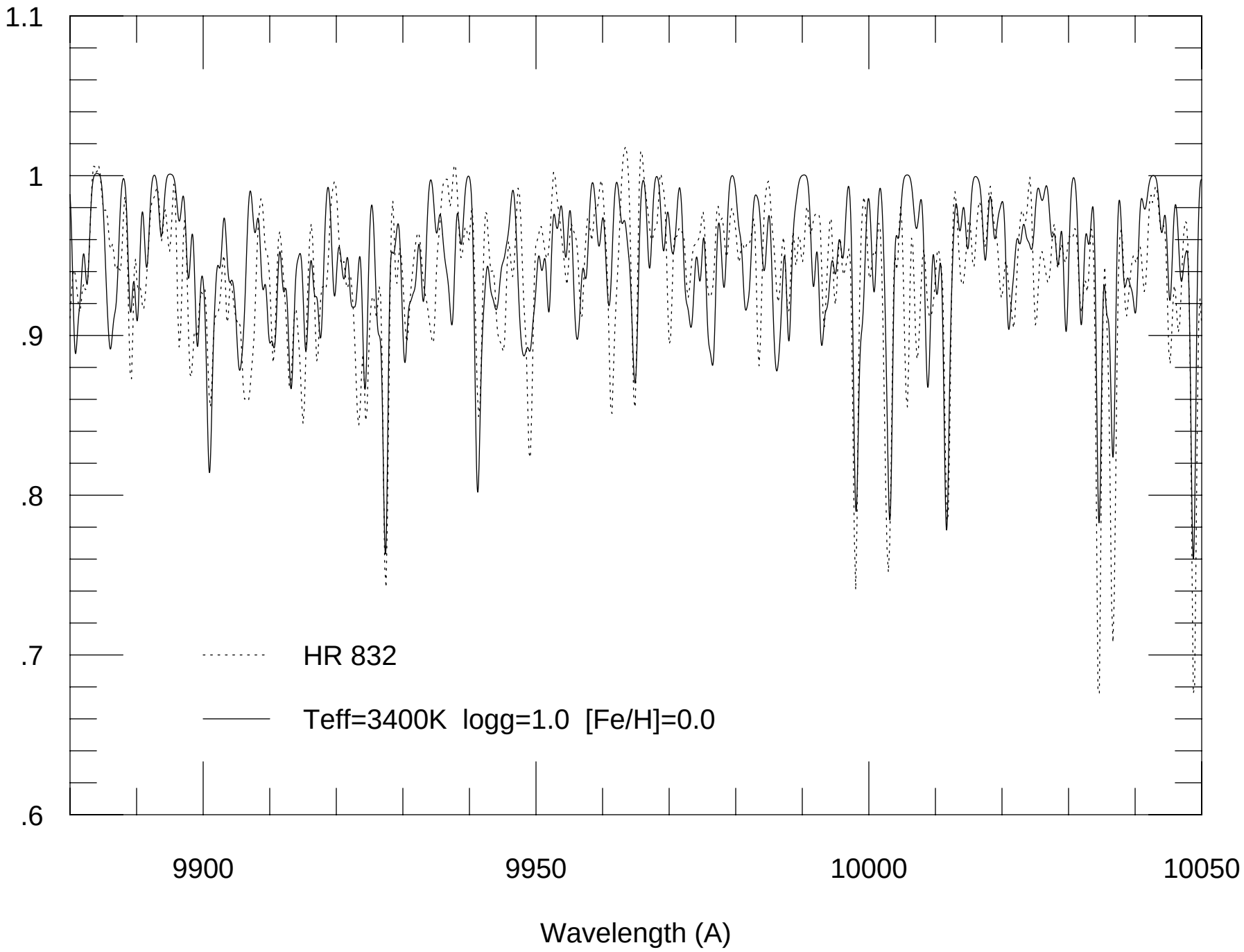
1.1
1
.9
.8
.7
.6
9900
9950
10000
10050
Wavelength (A)
HR 832
Teff=3400K logg=1.0 [Fe/H]=0.0

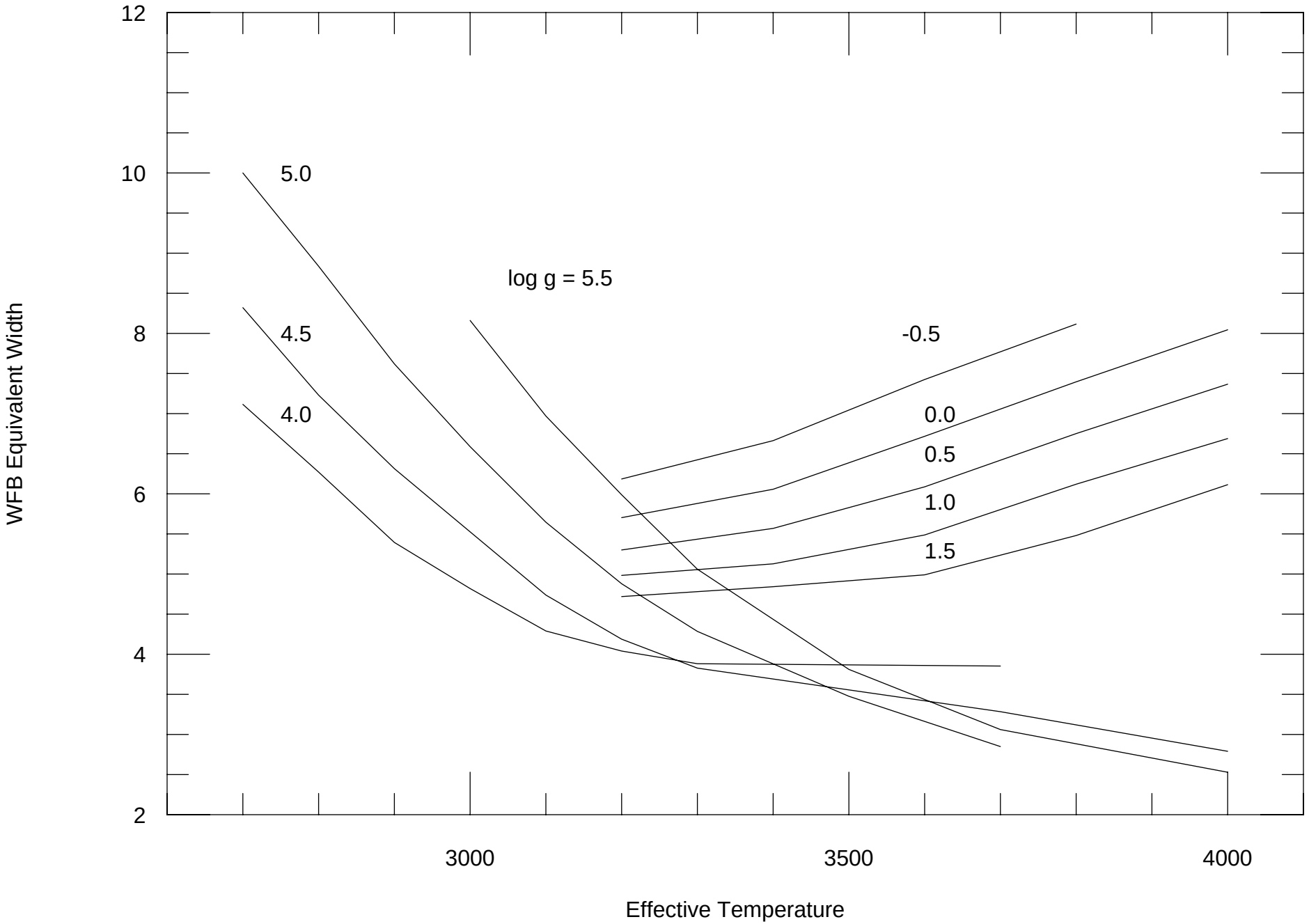
12
10
8
6
4
2
WFB Equivalent Width
log g = 5.5
5.0
4.5
4.0
-0.5
0.0
0.5
1.0
1.5
3000
3500
4000
Effective Temperature

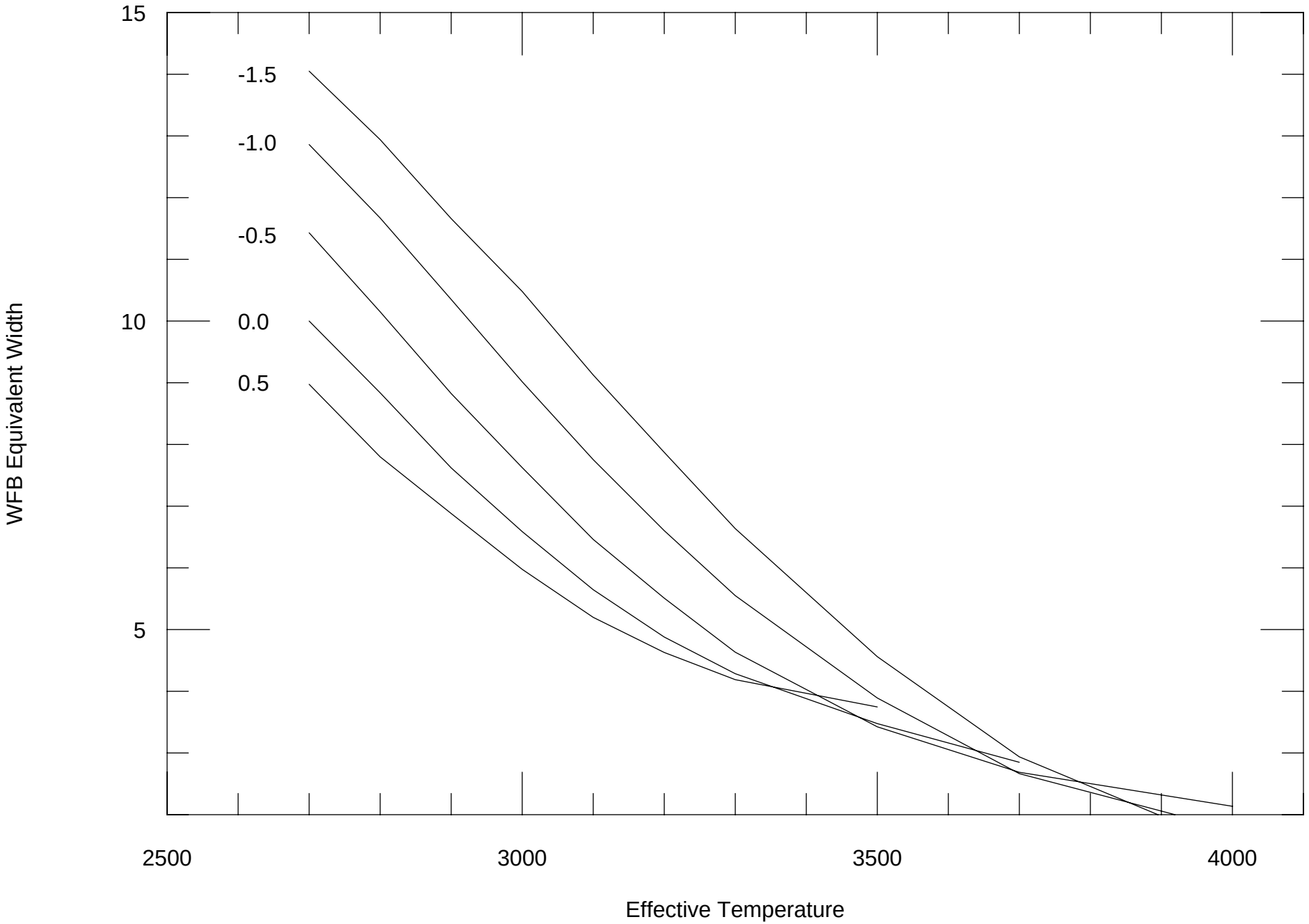
15
10
5
-1.5
-1.0
-0.5
0.0
0.5
WFB Equivalent Width
2500
3000
3500
4000
Effective Temperature

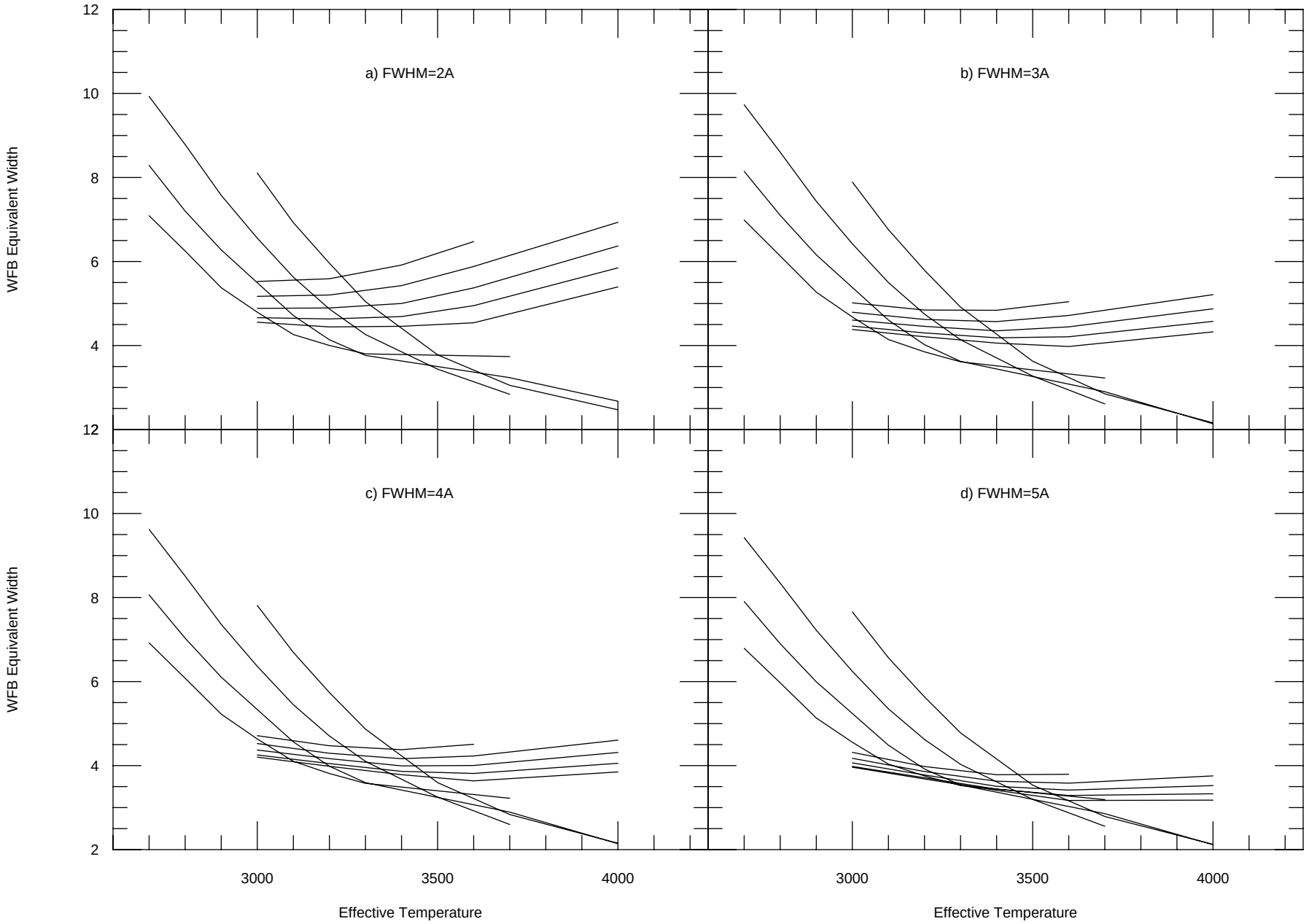
a) FWHM=2A
b) FWHM=3A
c) FWHM=4A
d) FWHM=5A
WFB Equivalent Width
WFB Equivalent Width
12
10
8
6
4
12
10
8
6
4
2
3000
3500
4000
3000
3500
4000
Effective Temperature
Effective Temperature